HHS Public Access

Author manuscript

J Mol Cell Cardiol. Author manuscript; available in PMC 2016 July 01.

Published in final edited form as:

J Mol Cell Cardiol. 2015 July ; 84: 52–60. doi:10.1016/j.yjmcc.2015.04.010.

REGIONAL VARIATION OF THE INWARDLY RECTIFYING POTASSIUM CURRENT IN THE CANINE HEART AND THE CONTRIBUTIONS TO DIFFERENCES IN ACTION POTENTIAL REPOLARIZATION

Jonathan M. Cordeiro[1], **Tanya Zeina**[1], **Robert Goodrow**[1], **Aaron D. Kaplan**[3], **Lini M. Thomas**[1], **Vladislav V. Nesterenko**[1], **Jacqueline A. Treat**[1], **Leo Hawel III**[2], **Craig Byus**[2], **Glenna C. Bett**[3,4], **Randall L. Rasmusson**[3], and **Brian K. Panama**[1]

[1]Department of Experimental Cardiology, Masonic Medical Research Laboratory, Utica, NY

[2]Division of Biomedical Sciences, School of Medicine, University of California, Riverside, Riverside, CA

[3]Department of Physiology and Biophysics, State University of New York, University of Buffalo, Buffalo, NY

[4]Department of Obstetrics and Gynecology, State University of New York, University of Buffalo, Buffalo, NY

Abstract

Background—The inward rectifier potassium current, I_{K1}, contributes to the terminal phase of repolarization of the action potential (AP), as well as the value and stability of the resting membrane potential. Regional variation in I_{K1} has been noted in the canine heart, but the biophysical properties have not been directly compared. We examined the properties and functional contribution of I_{K1} in isolated myocytes from ventricular, atrial and Purkinje tissue.

Methods and Results—APs were recorded from canine left ventricular midmyocardium, left atrial and Purkinje tissue. The terminal rate of repolarization of the AP in ventricle, but not in Purkinje, depended on changes in external K^+ ($[K^+]_o$). Isolated ventricular myocytes had the greatest density of I_{K1} while atrial myocytes had the lowest. Furthermore, the outward component of I_{K1} in ventricular cells exhibited a prominent outward component and steep negative slope conductance, which was also enhanced in 10 mM $[K^+]_o$. In contrast, both Purkinje and atrial cells exhibited little outward I_{K1}, even in the presence of 10 mM $[K^+]_o$, and both cell types showed more persistent current at positive potentials. Expression of Kir2.1 in the ventricle was 76.9-fold

Corresponding author: Brian K. Panama, PhD, Department of Experimental Cardiology, Masonic Medical Research Laboratory, 2150 Bleecker Street, Utica, NY 13501, Phone: (315) 735-2217 x125, Fax: (315) 735-5648, panamab@mmrl.edu.

Disclosures: Drs. Bett and Rasmusson are founders and have equity interests in Cytocybernetics, Inc.

higher than that of atria and 5.8-fold higher than that of Purkinje, whereas the expression of Kir2.2 and Kir2.3 subunits was more evenly distributed in Purkinje and atria. Finally, AP clamp data showed distinct contributions of I_{K1} for each cell type.

Conclusions—I_{K1} and Kir2 subunit expression vary dramatically in regions of the canine heart and these regional differences in Kir2 expression likely underlie regional distinctions in I_{K1} characteristics, contributing to variations in repolarization in response to in $[K^+]_o$ changes.

Keywords

ventricle; Purkinje; electrophysiology; atria; potassium channel

1. INTRODUCTION

Repolarization of the cardiac action potential (AP) is controlled by several voltage-dependent K^+ currents. In the canine ventricle, four K^+ currents play important roles in controlling the cardiac action potential duration[1–5]: (i) a Ca^{2+}-independent transient outward K^+ current (I_{to1}) (in contrast to the Ca^{2+}-dependent current, I_{to2}[6]); (ii) a rapid and slow delayed rectifier K^+ current (I_{Kr} and I_{Ks}, respectively) and (iii) an inwardly rectifying K^+ current (I_{K1}). I_{K1} has been identified in the myocardium of most mammalian species (for review see [7, 8]), but the density of I_{K1} among different species as well as among different cardiac tissue types is highly variable [9–11]. Previous studies have shown that the I_{K1} density is large in the ventricle, small in atria and largely absent in sinoatrial node [12–14].

The salient features of I_{K1}, such as its negative slope conductance and the crossover of the I-V relation upon increases in external K^+ have long been identified[15], and their physiological significance has been extensively studied [16, 17] (see Trautwein[18]). The strong rectification of I_{K1} is the result of voltage-dependent block by intracellular Mg^{2+} [19] and polyamines [20], primarily spermine and spermidine[21]. The channels that carry cardiac I_{K1} belong to the Kir2.x subfamily, namely Kir2.1 through Kir2.3[8, 22]. Each Kir2 channel is composed of four subunits which form monomeric channels, although native I_{K1} channels likely exist as heteromultimers[23–25]. When expressed in mammalian cells, all Kir2.x channels exhibit properties that are similar to native I_{K1} [10], although each Kir2.x channel has a different current profile[10], reflecting the differences in polyamine induced rectification[26]. For example, Kir2.1 and Kir2.2 channels show a prominent negative slope conductance and rectify ‘completely’ above −20 mV, while Kir2.3 channels pass significant current at these potentials [10]. The distinct properties of different Kir2.x channels have been implicated in regional and species differences in I_{K1}, as observed in sheep heart where the incomplete rectification of I_{K1} in atria is attributed to the predominant expression of Kir2.3[10]. Furthermore, individual reports [27–29] indicate the I_{K1} in canine heart appears to differ among ventricular, Purkinje and atrial myocytes. However, I_{K1} has never been directly compared between these three tissue types.

Since the canine heart is used as both a model for safety pharmacology and to stimulate cardiac electrophysiological diseases, such as atrial fibrillation[30], Long QT[31, 32] and Brugada Syndromes[33], the present study compares the electrophysiological and molecular constituents of I_{K1} in single myocytes isolated from the canine heart. Here we show that the

maximal rate of repolarization of the AP strongly depends on external K^+ ($[K^+]_o$) in ventricle, but not in Purkinje. We also show that the biophysical and molecular properties of I_{K1} differ between ventricular, Purkinje and atrial cells. While Kir2.1 is highly expressed in the ventricle, the other putative Kir2 subunits, Kir2.2 and Kir2.3, were more equally distributed in the three cardiac tissue types. Taken together, our data suggest that prominent differences in the expression Kir2 subunits and the characteristics of I_{K1} contribute to the differences of AP repolarization and its response to $[K^+]_o$ among atrial, ventricular and Purkinje tissues.

2. MATERIALS AND METHODS

2.1 Isolated tissue action potential recordings

This investigation conformed to the Guide for the Care and Use of Laboratory Animals published by the National Institutes of Health (Eighth Edition, 2011), and all protocols were approved by the Animal Care and Use Committee at the Masonic Medical Research Laboratory, and hearts from 39 total canines were used in the study. The mongrel canines of either sex were anti-coagulated with heparin and anesthetized with pentobarbital (30–35 mg/kg, i.v.). The chest was opened via left thoracotomy, the heart excised, placed in a cardioplegic solution (4 °C-Tyrode's solution with 12 mM $[K^+]_o$). Left ventricle midmyocardial (Mid-LV) (approximately 1.0 × 0.5 × 0.1 cm), left atrial tissue and Purkinje tissue were isolated from hearts. The preparations of ventricle consisted of dermatome shavings (Davol Simon Dermatome Power Handle 3293 with cutting head 3295, Cranston, R.I.) obtained from the left ventricular free wall. The tissues were superfused with oxygenated (95% O_2/5% CO_2) Tyrode's solution maintained at 36–37 °C. The composition of the Tyrode's solution was (in mM): NaCl 129, KCl 5.4, NaH_2PO_4 0.9, $NaHCO_3$ 20, $CaCl_2$ 1.8, $MgSO_4$ 0.5, and D-Glucose 5.5; pH=7.4. All preparations were allowed to equilibrate until the action potentials achieved steady-state (usually 3–4 hours). The tissues were stimulated at basic cycle lengths (BCL) ranging from 1000 and 2000 ms using rectangular stimuli (2–5 ms duration, 2–2.5 times diastolic threshold intensity) delivered through thin silver bipolar electrodes. Transmembrane action potentials were recorded from the two tissues simultaneously using glass microelectrodes filled with 2.7 M KCl (10–30 Mohms: DC resistance) connected to a high input-impedance amplification system (Electro 705 Electrometer, World Precision Instruments). The signals were digitized (model 1401 AD/DA system, Cambridge Electronic Designs [C.E.D.]) and analyzed (Spike 2 acquisition and analysis module, C.E.D.).

2.2 Isolation of canine cardiomyocytes

Left ventricular or left atrial preparations were dissected and cells dissociated as described previously[3]. For isolation of mid-left ventricular cells (Mid-LV), thin slices of tissue from the Epi and Endo were shaved from the wedge using a dermatome to expose the midmyocardium, and the midmyocardium was subsequently shaved and removed for further digestion. For atrial cells, the pectinate and appendage muscle were isolated. The tissue was then agitated in the enzyme solution at 37 °C for cell dissociation. Canine Purkinje cells were isolated using techniques previously described [34]. Briefly, Purkinje fibers from both ventricles were dissected out and placed in a small dish. Fibers were then subjected to

enzyme digestion with the nominally Ca^{2+}-free solution supplemented with 1.0 mg/ml collagenase (Type II, Worthington) and 30 mM 2,3-butanedione monoxime (Sigma-Aldrich) at 36 °C. Dissociation of cells from the fibers was aided by agitation of the enzyme solution with a small stir bar. Periodically, enzyme solution containing Purkinje cells in suspension was removed and added to a modified storage solution. Fresh enzyme solution was added to the undigested Purkinje fibers to maintain a volume of about 2 ml. Digestion of the Purkinje fibers into individual myocytes typically required 15–35 min. The cells were kept in the 0.1 mM Ca^{2+} solution at room temperature until use.

2.3 Single cell electrophysiology

Voltage-clamp recordings were made using a MultiClamp 700A amplifier and MultiClamp Commander (Molecular Devices, Foster City, CA). Patch pipettes were fabricated from borosilicate glass capillaries (1.5 mm O.D., Fisher Scientific, Pittsburgh, PA). The pipettes were pulled using a gravity puller (Narishige, Tokyo, Japan) and the pipette resistance ranged from 1–3 MΩ. The cardiomyocytes were superfused with a HEPES Buffer of the following composition (mM): NaCl 135, KCl 5.4, $MgCl_2$ 1.0, $CaCl_2$ 1.8, HEPES 10, NaH_2PO_4 0.33 and D-Glucose 10, pH adjusted to 7.4 with NaOH. The patch pipette solution (K_{INT}) had the following composition (mM): K-aspartate 125, KCl 10, $MgCl_2$ 1.0, EGTA 5, MgATP 5, HEPES 10, NaCl 10, pH=7.2 with KOH. All experiments were performed at 37 °C. After a whole-cell patch was established cell capacitance was measured by applying −5 mV voltage steps. Series resistance was compensated to 60–70%. All analog signals were acquired at 10–50 kHz, filtered at 4–6 kHz and digitized with a Digidata 1322 converter (Molecular Devices). I_{K1} currents were elicited by step increments of 10 mV between −120 and 0 mV from a holding potential of −80 mV and currents were evaluated at the end of the 500-ms step pulse, in the absence and presence of 100 μM $BaCl_2$, where I_{K1} was considered to be the Ba^{2+}-sensitive current. For analysis of kinetics of I_{K1} activation, hyperpolarizing steps down to −110 mV were applied to the cells in 10 mV decrements from a holding potential of −30 mV. The P/5 method was used to subtract the capacitance transient from fast activating I_{K1} currents, or K^+-free HEPES buffer was rapidly eliminate I_{K1} in order to isolate it from the capacitance currents, as similarly performed in Panama et al[11]. For action potential clamp experiments, pre-recorded action potentials from ventricular, Purkinje and atrial myocytes served as voltage waveforms. Action potentials of single cells were recorded using whole cell patch pipettes. The resistance of the electrodes was 1–3 Mohm when filled with the K_{INT} pipette solution. Action potentials were elicited using a 3 ms current pulse at 120% threshold amplitude.

2.4 Electronic Expression of I_{K1}

The electronic expression of I_{K1} was performed in the whole cell configuration, similarly as previously described[35] using a Cybercyte system (Cytocybernetics Inc., Pendleton, NY). I_{K1} I-V relations for Mid-LV and Purkinje were fit with the following function:

$$I_{K1}=G\times\left(g_{K1}\times\frac{V_m-V_{rev}}{1+\exp\left(k^{-1}\times\left(V_m-V_{\frac{1}{2}}\right)\right)}+g_{linear}\times(V_m-V_{rev})\right)$$

Cells were bathed in Tyrode solution and experiments were conducted at room temperature for increased patch stability. Model parameters were fit by adjusting g, g_{K1}, g_{linear} V_{rev}, $V_{1/2}$, and k to experimental data manually using a visual goodness of fit procedure, comparisons of data and model currents are given in the Supplementary figure 1S. Subtraction of currents was obtained by using a negative conductance using a model for I_{K1} from the 5.4 mM ventricular parameters, similar to that used for other ionic current cancelling procedures[36–38]. Differing I_{K1} models were simulated on a separate computer and added in as a command current[35].

2.5 Analysis of mRNA expression

Tissue was washed in Tyrode's solution and immediately frozen in liquid nitrogen before storage at −80 °C. For RNA isolation, the tissue was disrupted with a mortar and pestle and then homogenized with a sterile syringe and needle. After homogenization, the RNeasy Fibrosis Tissue kit was used to isolate the RNA (Qiagen). A NanoDrop® spectrophotometer (Thermo Scientific) was used to quantify RNA samples. Samples were treated with DNase I to remove contaminating genomic DNA. The Superscript™ III Reverse Transcriptase kit (Life Technologies) approach was used to synthesize cDNA from 1–5 μg of RNA, exactly according to the manufacturer protocol. cDNA synthesis reactions were run without reverse transcriptase (-RT) showed no amplification (Supplementary Figure 2S), indicating genomic DNA was not affecting the quantification.

Both SYBR green® and TaqMan systems (Life Technologies) used.

Probes sets:

KCNJ2- Cf03022918_s1 – TaqMan FAM (Life Technologies)

KCNJ12- Cf02713141_s1 – TaqMan FAM (Life Technologies)

KCNJ4 – Forward 5′ GGACTTTGAGATCGTGGTCA 3′; Reverse 5′ CGCGAGTAGTCCACCTTGTA 3′ – SYBR Green

18S rRNA- Forward 5′ TCCGACTTTCGTTCTTGATTAATG 3′; Reverse 5′ CGCCGCTAGAGGTTGAAATTC 3′ – SYBR Green

Maxima SYBR Green and Maxima Probe ROX master mixes (Thermo Scientific) were used for SYBR Green oligos and TaqMan probes, respectively, in the amplification reaction. A Real-Time thermal cycler PCR System 7000 (Life Technologies) was used to amplify the particular gene amplicons from the cDNA. All no template control wells, containing the reaction mix but water instead of cDNA, were negative in all PCR runs. The mRNA levels were referenced to 18S rRNA. For relative quantification, the ΔΔCt method was used [39].

2.6 Analysis of polyamine concentrations

Tissues were washed in HEPES Buffer, gently blotted dry and weighed. The samples were minced in RNase free water (2 ml/gram of tissue) and homogenized in a 50 ml conical tube, followed by a spin for 2 minutes at 3000g. The supernatant was transferred to a 1 ml tube and centrifuged for 15 minutes at 11,500g. Exactly 100 μl of supernatant was removed for later protein quantification. The remaining supernatant was transferred to a clean tube and

perchloric acid was added to make a 0.2 N final concentration. Following thorough mixing, the sample was incubated for 10 minutes at room temperature. After, the sample was centrifuged for 10 minutes at 11,500g. The supernatant was removed and stored at −80 °C. Polyamines spermine, spermidine and putrescine were quantified by HPLC, as described previously[40].

2.7 Data and statistical analysis

Data are presented as mean ± SEM. Statistical comparisons were made using paired or unpaired Student's t-test when appropriate. A one-way ANOVA was used for multiple comparisons, and $p<0.05$ was considered statistically significant (*). The V_{min} was obtained finding the minimum of derivative (dV/dt) of the AP, excluding the first 50 ms after AP upstroke. For atrial cells, the dV/dt was continuously decreasing, and thus a reliable minimum could not be obtained.

3. RESULTS

3.1 Action potential recordings from different regions of the canine heart

The canine heart is used as a model in pharmacological safety testing and experimental cardiac electrophysiology, and extracellular K^+ ($[K^+]_o$) is often varied to mimic pathophysiological hypo- or hyperkalemic states. We recorded APs from Mid-LV, atrial and Purkinje tissue at a pacing rate of 0.5 Hz (Figure 1) under different concentrations of $[K^+]_o$. As expected, APs in all tissue types decreased with an increase in $[K^+]_o$ from 5.4 to 10 mM and increased in the presence of 2 mM $[K^+]_o$ ($p<0.05$) in addition to hyperpolarization of the resting membrane potential, as previously noted[41] (Table 1). The beat to beat variability was minimal, as shown in Supplementary Figure 3S. The V_{min}, which is an indicator of the maximal terminal rate of repolarization, also increased with elevations $[K^+]_o$ for Mid-LV but not Purkinje tissue (Figure 2A). V_{min} for atria could not be reliably measured since V_{min} was continuously decreasing. Similar differences in V_{min} were obtained for a pacing rate of 1 Hz (−1.39 ± 0.19 and −0.71 ± 0.11 V/s for Mid-LV and Purkinje, respectively (n=5 for each; $p<0.05$) (Supplementary Table 1S).

3.2 Action potential recordings from single cells

To compare the AP changes observed in tissue to those of isolated myocytes, we recorded from Mid-LV, atrial and Purkinje cells at a pacing rate of 0.5 Hz. Figure 1B shows representative AP records obtained from a Mid-LV cell when the $[K^+]_o$ was again varied from normal (5.4 mM) to 2 mM and then to 10 mM, as well as AP recordings from a Purkinje and atrial cell, respectively, following the same changes in $[K^+]_o$. As seen with tissue experiments, Purkinje cells exhibited a more prominent phase 1 repolarization and had a longer AP. Following exposure to 10 mM $[K^+]_o$, the APD of all cell types markedly shortened; however, the degree of APD shortening was greatest in Purkinje cells, as seen in tissue experiments. Exposure of all cell types to 2.0 mM $[K^+]_o$ resulted in prolongation of the APD. Importantly, like that of tissue, the V_{min} strongly changed with $[K^+]_o$ in Mid-LV myocytes but not for Purkinje (Fig. 2B). Taken together, the AP parameters from the isolated myocytes paralleled those from tissue, both of which showed stark differences in the terminal phase of repolarization.

3.3 I_{K1} recordings from different regions of the canine heart

The AP data in both myocytes and tissue showed that the rate of terminal repolarization is different in the three cell types. Since I_{K1} strongly contributes to the late phase of repolarization of the AP and shifts proportionally with the $[K^+]_o$ we hypothesized that the magnitude, and perhaps the biophysical properties, of I_{K1} is different in each cell type. We measured I_{K1} by application of square-wave voltage-clamp pulses (Figure 3). Large steady-state inward currents could be observed in Mid-LV cells, whereas intermediate sized currents were found in Purkinje cells in response to hyperpolarizing voltage, and currents were smallest in atrial cells. Analysis of the I-V relation shows that I_{K1} is largest in ventricle and smallest in atria (−26.7 ± 2.8, −9.0 ± 3.4, and −2.6 ± 0.32 pA/pF at −120 mV for ventricular, Purkinje, and atrial, respectively (p<0.05)). In addition, the outward component of Mid-LV I_{K1} showed a prominent negative slope and rectified 'completely,' meaning that only a very small current persisted at depolarized potentials (0.26 ± 0.14 pA/pF at 0 mV for Mid-LV). On the other hand, the outward component of I_{K1} in Purkinje and atrial showed a weak negative slope and persistent current at depolarized potentials ((1.4 ± 0.79 and 0.5 ± 0.14 pA/pF at 0 mV for Purkinje and atria, respectively).

3.4 I_{K1} in response to changes in $[K^+]_o$

Given the differences in I_{K1} rectification among the three cell types we wondered how I_{K1} would change with changes in $[K^+]_o$. Whole cell currents were activated by a step to −10 mV followed by a 500-ms ramp to −120 mV from a holding potential of −80 mV. No blockers were added to the recording solution as the activation pulse would activate and eliminate Na^+ (I_{Na}) and Ca^{2+} currents (I_{Ca}). Similar to results using square wave pulses, the inward current at the end of the ramp was largest in Mid-LV cells, intermediate in Purkinje cells and smallest in atrial cells (Figure 4A). Furthermore, increasing $[K^+]_o$ increased the magnitude of inward I_{K1} in all 3 cell types. The lower panels (Figure 4B) show an enlargement of the outward component of I_{K1}. In Mid-LV cells, changing $[K^+]_o$ resulted in an increase in magnitude of I_{K1}, as previously described [7, 17, 42]. In contrast, Purkinje and atrial cells showed little increase in outward I_{K1} in response to the ramp protocol.

3.5 Kir2 mRNA and polyamine analysis in different regions of the canine heart

Previous studies have shown that homomeric channels formed by Kir2.1, 2.2 and 2.3 subunits each have different current profiles and polyamine induced rectification properties [26, 43]. The striking differences in I-V relations of I_{K1} seen in ventricular, Purkinje and atrial myocytes prompted us to investigate the differences in Kir2 subunit mRNA expression, as well as the polyamine concentrations, between the three regions. Kir2.1, 2.2 and 2.3 subunits were all expressed in the three regions, but the expression of Kir2.1 in the left ventricle was 76.9-fold higher than in atria (p<0.001) and 5.8-fold higher than in Purkinje (p<0.05) (Fig. 5). The expression of Kir2.2 and Kir2.3 subunits was more evenly distributed in Purkinje and atria. On the other hand, total polyamine concentrations were not different between ventricle and atria for spermine, spermidine and putrescine (Table 2). Polyamines in Purkinje tissue could not be measured due to small tissue amounts.

3.6 Kinetics of activation in canine cardiomyocytes

The weak negative slope seen in the I-V relations from Purkinje and atrial myocytes is reminiscent of the I-V relations from whole-cell recording of Kir2.3 channels expressed in HEK293 cells [26, 43]. We next determined whether the rate of I_{K1} activation (unblocking of polyamines) was different between the three cell types to assess the contribution of Kir2.3 subunits, which have slower activation rates. Hyperpolarizing steps were applied to the cells in 10 mV steps from a holding potential of −30 mV. As described previously[11, 20, 26], a double exponential was needed to fit the two components of activation: 1) a quasi-instantaneous activation and 2) slower activation which results from time-dependent polyamine unblock from the channels[20] (Figure 6). Ventricular myocytes had the fastest rate of time-dependent activation at −110 mV (1.56 ± 0.15 ms, n=7) while atrial myocytes had the slowest (13.1 ± 4.7 ms, n=5) (p<0.05). Purkinje (2.24 ± 0.14 ms, n=9) myocytes had I_{K1} which was slower (p<0.01) than that of ventricle.

3.7 Action potential clamp studies

Given the large differences in I_{K1} between the cell types, we evaluated the functional contribution of I_{K1} to the AP using the action potential clamp technique (Figure 7). Previously recorded ventricular, Purkinje and atrial cell action potentials served as the templates for the AP clamp experiments (Figure 7A). A train of 10 pulses were applied to the cell at a rate of 1 Hz in the absence and presence of 100 μM Ba^{2+}. Subtraction of the Ba^{2+} trace from the control trace resulted in the Ba^{2+}-sensitive difference current shown in Figure 7B. In LV-Mid cells, the outward component of I_{K1} in contributes 366.3±20.7 pA (n=8) or 1.86±0.05 pA/pF when normalized for cell size. In Purkinje cells, I_{K1} was 140.1±30.2 pA (n=5) or 0.62±0.11 pA/pF when normalized for cell size. In atrial cells, I_{K1} was 64.3±11.3 pA (n=7) or 0.48±0.06 pA/pF when normalized for cell size. Results show that while I_{K1} contributes predominantly to final portion of phase 3 in the cell types the profile of the outward component of I_{K1} was dramatically different. In atrial cells I_{K1} is likely influencing the AP at more positive potentials, because of the persistent I_{K1} outward current seen more depolarized voltages, which is consistent with the model proposed in Dhamoon et al[10] (see Discussion).

4. DISCUSSION

While the hallmark features of cardiac I_{K1} have been well characterized, such as the negative slope and ‘crossover’ effect upon increases $[K^+]_0$ (for review see references 44, 45 41), regional differences in I_{K1} have been noted in canine and other species. For example, we previously observed minimal changes in outward I_{K1} rabbit Purkinje myocytes in response to changes in $[K^+]_0$[9]. Furthermore, atrial-ventricular differences in I_{K1} have been noted in mouse[11], sheep[43] and human[46]. Since the canine heart is used as model for both safety pharmacology and for studying electrophysiological disorders, such as atrial fibrillation, Long QT[31, 32] and Brugada Syndromes[33], it is important to fully understand the regional differences in I_{K1}. As such, the novel findings of our study are as follows: **1)** the outward currents of I_{K1}, which until now have not been directly compared in canine, are different between ventricular, Purkinje and atrial myocytes, **2)** the outward component of current increased with $[K^+]_0$ in ventricle, while it did not in Purkinje or atria, **3)** the kinetics

of activation of I_{K1} is slower in Purkinje and atrial myocytes compared with those ventricle, and **4)** the contribution of I_{K1} is not limited to the terminal phase of repolarization in atrial myocytes (Figure 7).

Additionally, we found differences in the terminal phase of repolarization (V_{min}) in APs from canine ventricular and Purkinje tissue and myocytes at both normal and different $[K^+]_0$ (Table 1), and V_{min} changed with $[K^+]_0$ in ventricle but not in Purkinje (Fig. 2). We hypothesized that the shape and the lack of increase in the outward component of I_{K1} in Purkinje, in response to increases in $[K^+]_0$ (Fig. 4), could account for the nearly constant V_{min} despite increase of $[K^+]_0$ in this cell type/tissue. In support of this hypothesis, we synthetically applied different I_{K1} I-V relations[35] to Mid-LV cells and measured AP, using electronic expression of I_{K1}. Here we electronically subtracted the native I_{K1} and "expressed" our own synthetic I_{K1} which was modelled from previous Mid-LV I_{K1} recordings at different $[K^+]_0$. This technique gives us the ability to modulate only I_{K1} without changing other currents. Figure 8 shows the data for V_{min}, MDP, APD50 and APD90 for Mid-LV cells under the following conditions: Control (Con), subtracted I_{K1} ($-I_{K1}$), the I_{K1} I-V for Mid-LV at 5.4 mM K^+ ($+I_{K1}$ 5.4 mM K^+), the I_{K1} I-V for Mid-LV at 10 mM K^+ ($+I_{K1}$ 10 mM K^+) and the I_{K1} for Purkinje at 5.4mM K^+ ($+I_{K1}$ Purkinje). The V_{min} increased from −0.62 ± 0.01 V/s in $-I_{K1}$ to −1.39 ± 0.2 V/s and −2.35+0.23 V/s for $+I_{K1}$ 5.4 mM K^+ and $+I_{K1}$ 10 mM K^+, respectively ($p<0.01$). Consistent with Fig. 2, the Purkinje V_{min} was smaller than that of Mid-LV at 5.4 mM. The MDP was also more negative for $+I_{K1}$ 5.4 mM K^+ compared with $+I_{K1}$ 10 mM K^+, and with APD90 was increased with I_{K1} subtracted. Overall, the data show the cell specific I_{K1} properties are likely responsible for Purkinje and ventricular differences in the AP terminal rate of repolarization, as assessed by V_{min}.

Differences in Kir2.x subunit expression likely contribute to the regional variations in I_{K1}. We[26] and others[10, 47] previously showed that Kir2.x have different sensitivities to polyamines and have different rectification profiles with Kir2.1 and Kir2.2 channels passing outward current with a 'steep' negative slope and rectifying completely. On the other hand, the outward current profile from Kir2.3 channels has a more 'shallow' negative slope and does not rectify completely at positive potentials. In addition, under whole-cell recording conditions Kir2.1 outward currents increase with $[K^+]_0$ while currents from Kir2.3 channels do not show increases in outward current with $[K^+]_0$. These distinct properties of Kir2 channels have been attributed to atrial-ventricular difference in I_{K1}. For example, Dhamoon et al[48] showed that I_{K1} did not rectify completely in sheep atrial myocytes, which expressed Kir2.3 subunits predominantly, and the outward component of I_{K1} did not increase with elevations in $[K^+]_o$. However, in guinea pig atrial myocytes (which strongly express Kir2.1) I_{K1} showed an increase in outward currents in 10 mmol/L $[K^+]_o$.

Similar to Dhamoon et al, we found that the outward component of I_{K1} in Mid-LV myocytes showed a prominent negative slope and rectified 'completely,' whereas the outward component of I_{K1} in Purkinje and atrial showed a weak negative slope and persistent current at depolarized potentials. In addition, elevating $[K^+]_o$ in Mid-LV myocytes resulted in an increase in magnitude of outward I_{K1} and a 'cross-over' effect, as previously described [7, 17, 42], but Purkinje and atrial cells showed little, if any, increase in outward I_{K1}.

The mRNA expression of Kir2.1 in Mid-LV was 76.9-fold higher than that of atria and 5.8-fold higher than that of Purkinje. The large expression of Kir2.1 in the Mid-LV is consistent with steep negative slope profile of I_{K1} and the increase in current with elevations in $[K^+]_o$. On the other hand, mRNA of Kir2.2 and Kir2.3 subunits were more evenly distributed in Purkinje and atria. Therefore, we hypothesized that Kir2.3 channels are playing a greater role in Purkinje and atria since I_{K1}'s properties in these cell types are reminiscent of those seen from Kir2.3 current (i.e. lack of strong negative slope in the outward component and a lack of current increase with elevations in $[K^+]_o$). To understand the functional role of Kir2.3 subunits in Purkinje and atria, we measured the kinetics activation in all three cell types. Kir2.3 channel currents activate more slowly than those of Kir2.2 and Kir2.1 channels [26]. The rate activation is proportional to the number of Kir2.3 subunits in a heterotetrameric channel[11], and even the presence of one Kir2.3 subunit in a heteromeric channel (such as a Kir2.1–2.1–2.1–2.3 heterotetramer for example) slows activation[11]. Indeed the kinetics of activation was slower in Purkinje and atria when compared with Mid-LV, thus providing evidence for the role Kir2.3 subunits in generating distinct properties of I_{K1} in these two cell types.

As shown above in the AP and V_{min} data, the regional variation in I_{K1} contributes to differences in rate of the late phase of repolarization of the AP. It also likely that regional variation in I_{K1} contribute to differences in arrhythmia susceptibility between the three cell/tissue types. The data in Figure 7 show that while I_{K1} contributes predominantly to final portion of phase 3 in the cell types the profile of the outward component of I_{K1} is different in atrial cells, where I_{K1} contributes to the AP at positive potentials. Our experimental data largely agree with the model presented by Dhamoon[49], which suggests that a myocyte with "Kir2.3-like" properties (i.e. shallow negative slope and persistent current) will contribute to the plateau phase of the AP, in addition to the late phase of repolarization. Furthermore, data from Pogwizd[50] established that a robust I_{K1} current can prevent the development of delayed afterdepolarizations by stabilizing the membrane potential. However, a diminished I_{K1} (in myocytes from failing hearts for example) is less able to mitigate spontaneous membrane depolarizations. It is important to note that canine differs somewhat from that of human. For example, Jost et al[51] shows that I_{K1} in ventricle is more than 2-fold larger in canine verses human, and provides evidence that I_{K1} plays a greater role in the repolarization reserve in canine compared with human. In contrast, I_{K1} densities from human failing heart are only moderately less than canine (−6 pA/pF for human[52] verses −9 pA/pF at −120 mV). How these differences affect repolarization reserve and arrhythmia propensity will have to be examined in further investigations.

Several limitations and considerations exist in our study. First, it is important to note that while the terminal rate repolarization is highly dependent on I_{K1}, the AP durations (APD50 and 90) in Purkinje still change with elevations in $[K^+]_o$ despite the lack of change in outward current. This must be attributed to other K^+ currents, such as I_{Kr}, which are changing with $[K^+]_o$. Second, we did not perform protein analysis of Kir2.x subunits, which would provide further validation of the subunit expression between the three cell types, although the results can be explained by mRNA measurements. Third, we did not record single-channels from myocytes, which we believe would be complicated, since Kir2

channels can have multiple sub-levels[53] and single-channel conductances are altered by the number and particular Kir2.x isoform in a heteromeric channel, as we have shown previously[54]. Finally, intracellular polyamines likely also contribute to the regional variation between cell types. Despite the lack of differences in total polyamine content between ventricle and atria (Table 2), it is within the realm of possibility that differences in free intracellular polyamines[11] exist, which are not reliably quantifiable in these conditions.

In conclusion, I_{K1} and Kir2 subunit expression vary dramatically in regions of the canine heart, suggesting tissue-specific differences of Kir2 isoforms. Differences in the expression and properties of I_{K1} contribute to tissue-specific difference in AP characteristics, namely the terminal rate of repolarization, and their response to pathophysiological factors including variations in plasma K^+ concentration. The mechanisms underlying tissue-specific differences in expression of in I_{K1} will need to be addressed in future studies.

Supplementary Material

Refer to Web version on PubMed Central for supplementary material.

Acknowledgments

We thank Dr. Charles Antzelevitch for a thoughtful feedback on this manuscript. We are grateful to Judy Hefferon for technical assistance.

FUNDING SOURCES

This work was supported by grants from the National Institutes of Health [HL47678] (to Charles Antzelevitch) and the Free and Accepted Masons of the New York State, Florida, Massachusetts and Connecticut.

Reference List

1. Calloe K, Soltysinska E, Jespersen T, Lundby A, Antzelevitch C, Olesen SP, et al. Differential effects of the transient outward K^+ current activator NS5806 in the canine left ventricle. J Mol Cell Cardiol. 2010 Jan; 48(1):191–200. [PubMed: 19632239]
2. Calloe K, Nof E, Jespersen T, Olesen SP, Di Diego JM, Chlus N, et al. Comparison of the effects of the transient outward potassium channel activator NS5806 on canine atrial and ventricular cardiomyocytes. J Cardiovasc Electrophysiol. 2011 Sep 1; 22(9):1057–66. [PubMed: 21457383]
3. Cordeiro JM, Calloe K, Moise NS, Kornreich B, Giannandrea D, Di Diego JM, et al. Physiological consequences of transient outward K+ current activation during heart failure in the canine left ventricle. J Mol Cell Cardiol. 2012 Jun 1; 52(6):1291–8. [PubMed: 22434032]
4. Calloe K, Goodrow R, Olesen SP, Antzelevitch C, Cordeiro JM. Tissue specific effects of acetylcholine in the canine heart. Am J Physiol Heart Circ Physiol. 2013 May 3; 305(1):H66–H75. [PubMed: 23645460]
5. Cordeiro JM, Panama BK, Goodrow R, Zygmunt AC, White C, Treat JA, et al. Developmental changes in expression and biophysics of ion channels in the canine ventricle. J Mol Cell Cardiol. 2013 Sep 10.64:79–89. [PubMed: 24035801]
6. Tseng GN, Hoffman BF. Two components of transient outward current in canine ventricular myocytes. Circ Res. 1989 Apr; 64(4):633–47. [PubMed: 2539269]
7. Nichols CG, Makhina EN, Pearson WL, Sha Q, Lopatin AN. Inward rectification and implications for cardiac excitability. Circ Res. 1996; 78:1–7. [PubMed: 8603491]
8. Lopatin AN, Nichols CG. Inward rectifiers in the heart: an update on I(K1). J Mol Cell Cardiol. 2001 Apr; 33(4):625–38. [PubMed: 11273717]

9. Cordeiro JM, Spitzer KW, Giles WR. Repolarizing K^+ currents in rabbit heart Purkinje cells. J Physiol. 1998 May 1; 508(Pt 3):811–23. [PubMed: 9518735]
10. Dhamoon AS, Pandit SV, Sarmast F, Parisian KR, Guha P, Li Y, et al. Unique Kir2.x properties determine regional and species differences in the cardiac inward rectifier K^+ current. Circ Res. 2004 May 28; 94(10):1332–9. [PubMed: 15087421]
11. Panama BK, McLerie M, Lopatin AN. Heterogeneity of IK1 in the mouse heart. Am J Physiol Heart Circ Physiol. 2007 Dec; 293(6):H3558–H3567. [PubMed: 17890431]
12. Giles WR, Imaizumi Y. Comparison of potassium currents in rabbit atrial and ventricular cells. J Physiol (Lond). 1988; 405:123–45. [PubMed: 2855639]
13. Hume JR, Uehara A. Ionic basis of the different action potential configurations of single guinea-pig atrial and ventricular myocytes. J Physiol (Lond). 1985; 368:525–44. [PubMed: 2416918]
14. Irisawa H, Brown HF, Giles WR. Cardiac pacemaking in the sinoatrial node. Physiol Rev. 1993; 73:197–227. [PubMed: 8380502]
15. Shah AK, Cohen IS, Datyner NB. Background K+ current in isolated canine cardiac Purkinje myocytes. Biophys J. 1987; 52:519–25. [PubMed: 2445390]
16. Hutter OF, Noble D. Rectifying properties of heart muscle. Nature. 1960 Nov 5.188:495. [PubMed: 13717088]
17. Shimoni Y, Clark RB, Giles WR. Role of an inwardly rectifying potassium current in rabbit ventricular action potential. J Physiol. 1992; 448:709–27. [PubMed: 1593485]
18. Trautwein W. Membrane currents in cardiac muscle fibers. Physiol Rev. 1973 Oct 1; 53(4):793–835.
19. Matsuda H, Saiguse A, Irisawa H. Ohmic conductance through the inwardly rectifying K^+ channel and blocking by internal Mg^{2+} Nature. 1987; 325:156–9. [PubMed: 2433601]
20. Lopatin AN, Makhina EN, Nichols CG. Potassium channel block by cytoplasmic polyamines as the mechanism of intrinsic rectification. Nature. 1994 Nov 24; 372(6504):366–9. [PubMed: 7969496]
21. Lopatin AN, Shantz LM, Mackintosh CA, Nichols CG, Pegg AE. Modulation of potassium channels in the hearts of transgenic and mutant mice with altered polyamine biosynthesis. J Mol Cell Cardiol. 2000 Nov; 32(11):2007–24. [PubMed: 11040105]
22. Anumonwo JM, Lopatin AN. Cardiac strong inward rectifier potassium channels. J Mol Cell Cardiol. 2010 Jan; 48(1):45–54. [PubMed: 19703462]
23. Zobel C, Cho HC, Nguyen TT, Pekhletski R, Diaz RJ, Wilson GJ, et al. Molecular dissection of the inward rectifier potassium current (IK1) in rabbit cardiomyocytes: evidence for heteromeric co-assembly of Kir2.1 and Kir2.2. J Physiol. 2003 Jul 15; 550(Pt 2):365–72. [PubMed: 12794173]
24. Schram G, Pourrier M, Wang Z, White M, Nattel S. Barium block of Kir2 and human cardiac inward rectifier currents: evidence for subunit-heteromeric contribution to native currents. Cardiovasc Res. 2003 Aug 1; 59(2):328–38. [PubMed: 12909316]
25. Preisig-Muller R, Schlichthorl G, Goerge T, Heinen S, Bruggemann A, Rajan S, et al. Heteromerization of Kir2.x potassium channels contributes to the phenotype of Andersen's syndrome. Proc Natl Acad Sci U S A. 2002 May 28; 99(11):7774–9. [PubMed: 12032359]
26. Panama BK, Lopatin AN. Differential polyamine sensitivity in inwardly rectifying Kir2 potassium channels. J Physiol. 2006 Mar 1; 571(Pt 2):287–302. [PubMed: 16373386]
27. Cordeiro JM. K^+ current differences in Purkinje cells isolated from rabbit and dog heart. Biophysical Journal. 2005; 88:474a. Ref Type: Abstract.
28. Pinto JM, Boyden PA. Reduced inward rectifying and increased E-4031-sensitive K+ current density in arrhythmogenic subendocardial purkinje myocytes from the infarcted heart. J Cardiovasc Electrophysiol. 1998 Mar; 9(3):299–311. [PubMed: 9554735]
29. Melnyk P, Zhang L, Shrier A, Nattel S. Differential distribution of Kir2.1 and Kir2.3 subunits in canine atrium and ventricle. Am J Physiol Heart Circ Physiol. 2002 Sep; 283(3):H1123–H1133. [PubMed: 12181143]
30. Burashnikov A, Di Diego JM, Barajas-Martinez H, Hu D, Zygmunt AC, Cordeiro JM, et al. Ranolazine effectively suppresses atrial fibrillation in the setting of heart failure. Circ Heart Fail. 2014 Jul 1; 7(4):627–33. [PubMed: 24874201]

31. Davidenko JM, Cohen L, Goodrow RJ, Antzelevitch C. Quinidine-induced action potential prolongation, early afterdepolarizations, and triggered activity in canine Purkinje fibers. Effects of stimulation rate, potassium, and magnesium. Circulation. 1989 Jul.79:674–86. [PubMed: 2917391]
32. Gintant GA, Limberis JT, McDermott JS, Wegner CD, Cox BF. The canine Purkinje fiber: an in vitro model system for acquired long QT syndrome and drug-induced arrhythmogenesis. J Cardiovasc Pharmacol. 2001 May; 37(5):607–18. [PubMed: 11336111]
33. Calloe K, Cordeiro JM, Di Diego JM, Hansen RS, Grunnet M, Olesen SP, et al. NS5806 activates the transient outward potassium current in the canine ventricle and provides a new model of the Brugada syndrome. Biophys J. 2009; 96:666a. Ref Type: Abstract.
34. Dumaine R, Cordeiro JM. Comparison of K+ currents in cardiac Purkinje cells isolated from rabbit and dog. J Mol Cell Cardiol. 2007 Feb; 42(2):378–89. [PubMed: 17184792]
35. Bett GC, Kaplan AD, Lis A, Cimato TR, Tzanakakis ES, Zhou Q, et al. Electronic “expression” of the inward rectifier in cardiocytes derived from human-induced pluripotent stem cells. Heart Rhythm. 2013 Dec; 10(12):1903–10. [PubMed: 24055949]
36. Bot CT, Kherlopian AR, Ortega FA, Christini DJ, Krogh-Madsen T. Rapid genetic algorithm optimization of a mouse computational model: benefits for anthropomorphization of neonatal mouse cardiomyocytes. Front Physiol. 2012; 3:421. [PubMed: 23133423]
37. Workman AJ, Marshall GE, Rankin AC, Smith GL, Dempster J. Transient outward K+ current reduction prolongs action potentials and promotes afterdepolarisations: a dynamic-clamp study in human and rabbit cardiac atrial myocytes. J Physiol. 2012 Sep 1; 590(Pt 17):4289–305. [PubMed: 22733660]
38. Dong M, Sun X, Prinz AA, Wang HS. Effect of simulated I(to) on guinea pig and canine ventricular action potential morphology. Am J Physiol Heart Circ Physiol. 2006 Aug; 291(2):H631–H637. [PubMed: 16565319]
39. Livak KJ, Schmittgen TD. Analysis of relative gene expression data using real-time quantitative PCR and the $2^{-\Delta\Delta CT}$ Method. Methods. 2001 Dec; 25(4):402–8. [PubMed: 11846609]
40. Hawel L III, Byus CV. A streamlined method for the isolation and quantitation of nanomole levels of exported polyamines in cell culture media. Anal Biochem. 2002 Dec 15; 311(2):127–32. [PubMed: 12470671]
41. Noble D. Electrical properties of cardiac muscle attributable to inward going (anomalous) rectification. J Cell Comp Physiol. 1965 Dec; 66(Suppl 2):127–36.
42. Carmeliet E. Induction and removal of inward-going rectification in sheep cardiac Purkinje fibres. J Physiol. 1982 Jun.327:285–308. [PubMed: 6288926]
43. Dhamoon AS, Pandit SV, Sarmast F, Parisian KR, Guha P, Li Y, et al. Unique Kir2.x properties determine regional and species differences in the cardiac inward rectifier K+ current. Circ Res. 2004 May 28; 94(10):1332–9. [PubMed: 15087421]
44. Isenberg G. Cardiac purkinje fibers: cesium as a tool to block inward rectifying potassium currents. Pflugers Arch. 1976 Sep 30; 365(2–3):99–106. [PubMed: 988568]
45. Beeler GW, Reuter H. Voltage clamp experiments on ventricular myocardial fibers. J Physiol (Lond). 1970; 207:165–90. [PubMed: 5503866]
46. Wang Z, Yue L, White M, Pelletier G, Nattel S. Differential distribution of inward rectifier potassium channel transcripts in human atrium versus ventricle. Circulation. 1998 Dec 1; 98(22): 2422–8. [PubMed: 9832487]
47. Dhamoon AS, Jalife J. The inward rectifier current I_{K1} controls cardiac excitability and is involved in arrhythmogenesis. Heart Rhythm. 2005 Mar; 2(3):316–24. [PubMed: 15851327]
48. Dhamoon AS, Pandit SV, Sarmast F, Parisian KR, Guha P, Li Y, et al. Unique Kir2.x properties determine regional and species differences in the cardiac inward rectifier K+ current. Circ Res. 2004 May 28; 94(10):1332–9. [PubMed: 15087421]
49. Dhamoon AS, Pandit SV, Sarmast F, Parisian KR, Guha P, Li Y, et al. Unique Kir2.x properties determine regional and species differences in the cardiac inward rectifier K+ current. Circ Res. 2004 May 28; 94(10):1332–9. [PubMed: 15087421]
50. Pogwizd SM, Schlotthauer K, Li L, Yuan W, Bers DM. Arrhythmogenesis and contractile dysfunction in heart failure: Roles of sodium-calcium exchange, inward rectifier potassium

current, and residual beta-adrenergic responsiveness. Circ Res. 2001 Jun 8; 88(11):1159–67. [PubMed: 11397782]

51. Jost N, Virag L, Comtois P, Ordog B, Szuts V, Seprenyi G, et al. Ionic mechanisms limiting cardiac repolarization reserve in humans compared to dogs. J Physiol. 2013 Sep 1; 591(Pt 17): 4189–206. [PubMed: 23878377]
52. Han W, Zhang L, Schram G, Nattel S. Properties of potassium currents in Purkinje cells of failing human hearts. Am J Physiol Heart Circ Physiol. 2002 Dec; 283(6):H2495–H2503. [PubMed: 12388306]
53. Picones A, Keung E, Timpe LC. Unitary conductance variation in Kir2.1 and in cardiac inward rectifier potassium channels. Biophys J. 2001 Oct; 81(4):2035–49. [PubMed: 11566776]
54. Panama BK, McLerie M, Lopatin AN. Functional consequences of Kir2.1/Kir2.2 subunit heteromerization. Pflugers Arch. 2010 Oct; 460(5):839–49. [PubMed: 20676672]

Highlights

- I_{K1} and Kir2 subunit expression vary dramatically in different regions of the canine heart.
- The rate of repolarization of the action potential changes with external K^+ concentration in ventricle but not in Purkinje.
- The contribution of I_{K1} is not limited to the terminal phase of repolarization in atrial myocytes.

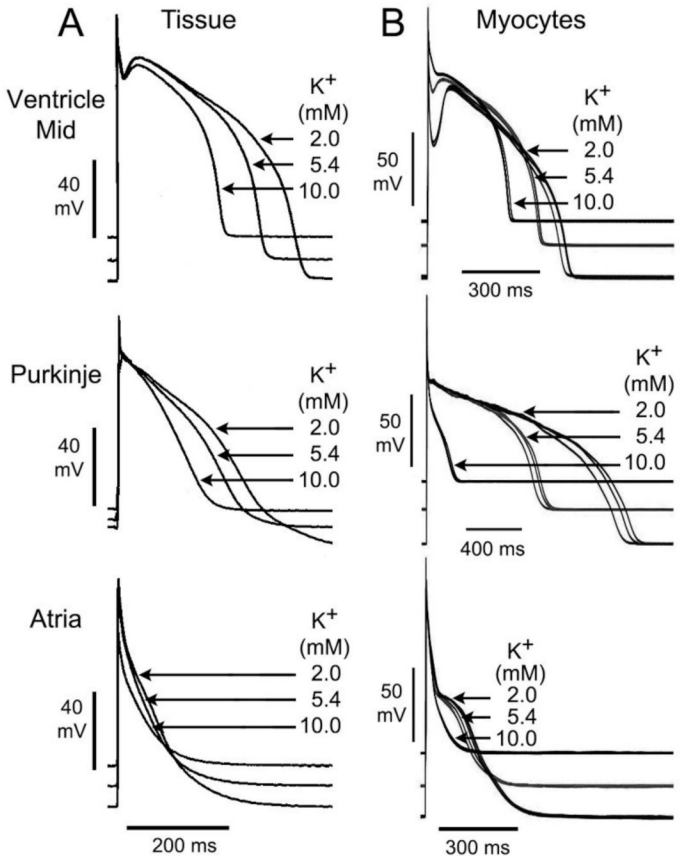

Figure 1. Representative action potentials from Mid-LV, Purkinje and atrial tissues and myocytes in different $[K^+]_o$ paced at 0.5 Hz

Action potentials for tissues (**A**) and myocytes (**B**) were characteristic of what has been previously observed. Several sweeps are shown for myocytes voltage clamp recordings.

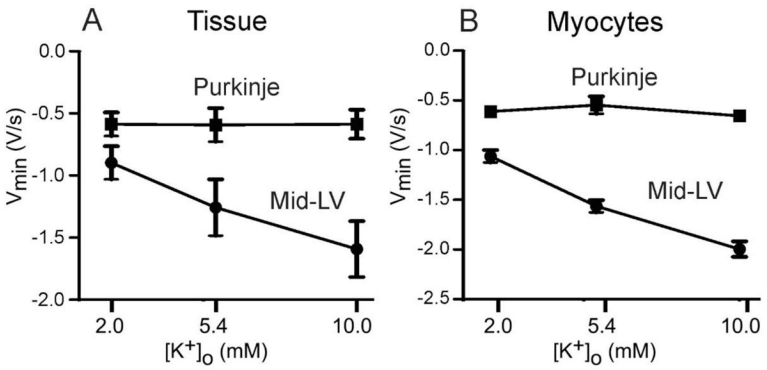

Figure 2. V_{min} dependence on $[K+]_0$ in tissue and cardiac myocytes

A. Plot of V_{min} vs. $[K^+]_0$. V_{min} changes with $[K^+]_0$ for ventricle but not Purkinje tissue. **B.** V_{min} vs. $[K^+]_0$. V_{min} changes with $[K^+]_0$ for ventricle but not Purkinje myocytes. (n=5; N=2 hearts for Mid-LV; n=3; N=3 hearts for Purkinje).

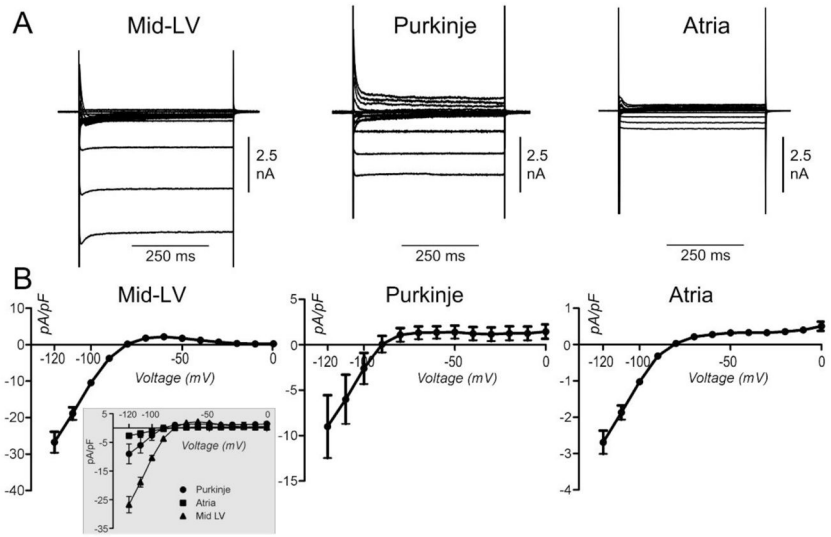

Figure 3. Whole cell currents from Mid-LV, Purkinje and atria myocytes at physiological K^+

A. Example current trances from Mid-LV, Purkinje and atria myocytes. Step increments of 10 mV between −120 and 0 mV from a holding potential of −80 mV **B.** Averaged current density vs. voltage plots for the Ba^{2+}-sensitive currents for the three cell types. (*Insert*: Averaged current density for all the cell types plotted on the same graph). n=10, N=7 hearts for Mid-LV; n=4, N=3 hearts for Purkinje; n=9, N=2 hearts for atria;

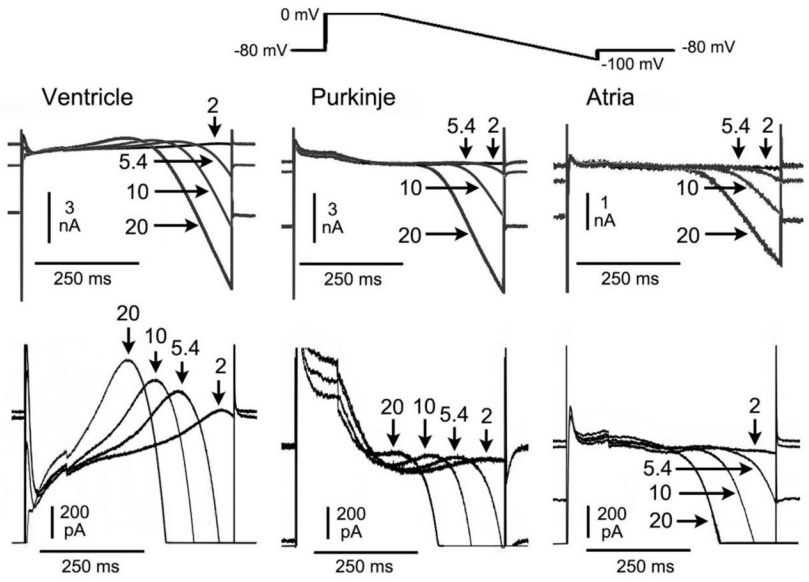

Figure 4. I_{K1} currents in different $[K^+]_0$ from cardiac myocytes

Representative currents for the three cell types in the presence of different external K^+ concentrations, 2, 5.4, 10 and 20 mM K^+. **A.** inward currents dramatically increase with elevations in K^+. **B.** the outward current component increases in Mid-LV cells with increasing K^+, but not in Purkinje and atrial cells.

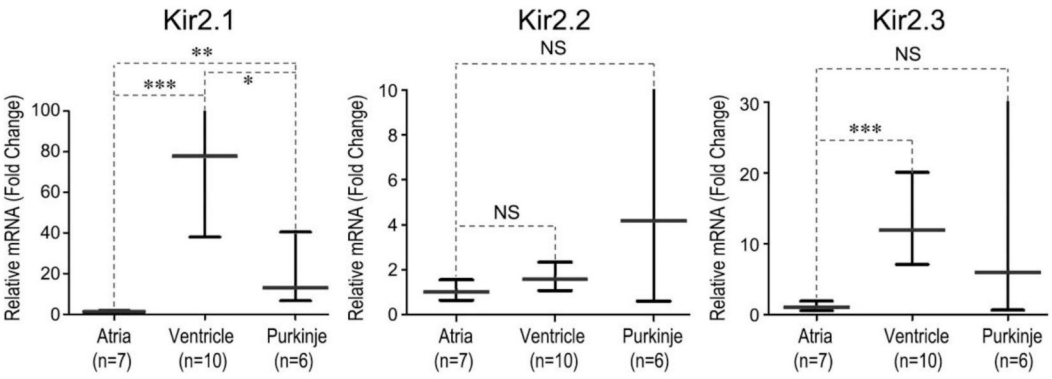

Figure 5. Kir2 subunit expression for Mid-LV, Purkinje and atria

The long horizontal bars represent the mean fold change and error bars denote the confidence interval (95%). The expression of Kir2.1 in the left ventricle was 76.9-fold higher than that of atria ($p<0.001$) and 5.8-fold higher than that of Purkinje ($p<0.05$).

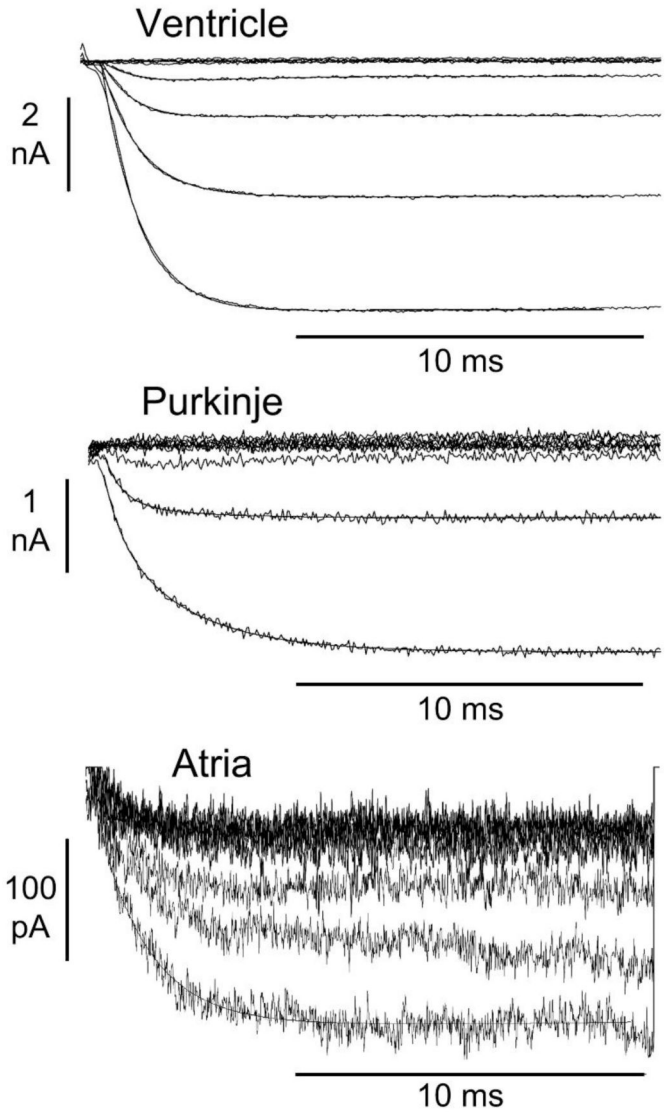

Figure 6. Kinetics of activation (unblock) from Mid-LV, Purkinje and atrial myocytes

Representative traces of I_{K1} in response to hyperpolarizing steps from Mid-LV, Purkinje and atrial myocytes, and double exponential fits are shown. At −110 mV slower tau values were 1.56 ± 0.15 ms (n=7), 2.24 ± 0.14 ms (n=9) and 13.1 ± 4.7 ms (n=5), for Mid-LV, Purkinje and atria, respectively. N=3, 5 and 5 hearts for Mid-LV, Purkinje and atria, respectively.

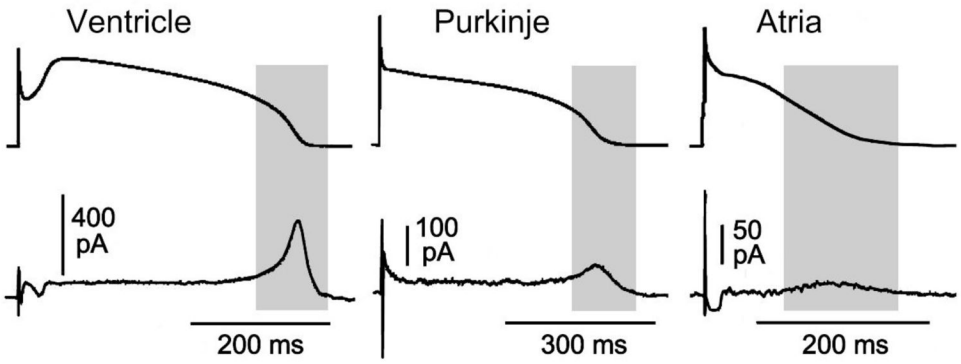

Figure 7. Action potential clamp waveforms and I_{K1} in cardiac myocytes

Top, previously recorded action potential waveforms from ventricular, Purkinje and atria myocytes were used as voltage protocols. *Bottom*, representative Ba^{2+} sensitive currents.

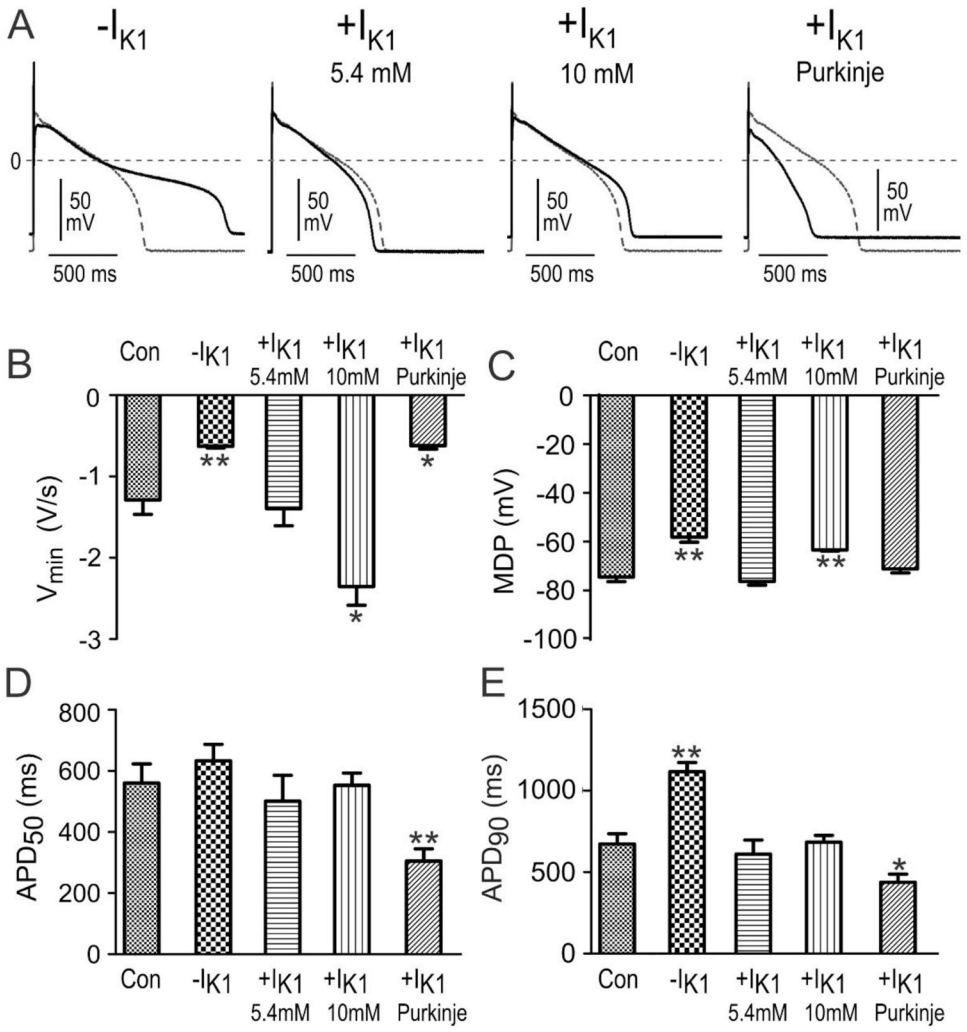

Figure 8. Electronic Expression of different I_{K1} profiles in Mid-LV cells

A. Representative AP with different synthetic I-V relations of I_{K1} recorded in the whole-cell configuration. The first panel shows an AP before and after subtraction of I_{K1}, the second panel shows the relative stability after both subtracting and adding I_{K1}, the third panels shows the effects of increasing I_{K1} in 10 mM $[K^+]_o$ (note this action only changes the inward rectifier), the fourth panel show the effects of using a Purkinje type current**. B.** Data for V_{min}, MDP, APD50 and APD90 for Mid-LV cells electronically expressing different properties of I_{K1}. Abbreviations: Control (Con), subtracted I_{K1} ($-I_{K1}$), the I_{K1} I-V for Mid-LV at 5.4 mM K^+ ($+I_{K1}$ 5.4 mM K^+), the I_{K1} I-V for Mid-LV at 10 mM K^+ ($+I_{K1}$ 10 mM K^+) and the I_{K1} for Purkinje at 5.4mM K^+ ($+I_{K1}$ Purkinje). n=5, N=1 heart.

Table 1

Action potential parameters from tissue in response to extracellular K^+ changes at 0.5 Hz pacing.

	Ventricle **N=4 hearts**	***Purkinje*** **N=4 hearts**	***Atria*** **N=5 hearts**
MDP (mV) 5.4 mM $[K+]_o$	−90.0±0.61	−89.2±1.7	−77.3±1.5*
MDP (mV) 2 mM $[K+]_o$	−98.3±1.0	−97.8±1.2	−86.6±2.6*
MDP (mV) 10 mM $[K+]_o$	−75.3±3.5	−77.9±0.9	−64.7±5.1
APD50 (ms) 5.4 mM $[K+]_o$	211±19.1	183±20.1	28.0±8.8*
APD50 (ms) 2 mM $[K+]_o$	252±43.6	232±38.6	36.8±9.7*
APD50 (ms) 10 mM $[K+]_o$	164±16.7	147±20.6	25.1±5.8*
APD90 (ms) 5.4 mM $[K+]_o$	275±17.7	307±55.3	123±15.1*
APD90 (ms) 2 mM $[K+]_o$	350±51.3	355±49.2	153±19.5*
APD90 (ms) 10 mM $[K+]_o$	199±14	217±27.9	102±14.4*

Abbreviations: MDP (mean diastolic potential), APD (action potential duration at 50 or 90 repolarization, APD50 and APD90.

* $p<0.05$ vs. ventricle

Table 2

Total polyamine concentrations in ventricular and atrial tissue.

	Spermine	Spermidine	Putrescine
Ventricle n=8 (nmol/mg protein)	1.54 ± 0.06	0.64 ± 0.05	0.19 ± 0.02
Atria n=7 (nmol/mg protein)	1.39 ± 0.15	0.59 ± 0.08	0.19 ± 0.03